# Characteristics of negative corona discharge in air at various gaps

Hongyu Sun[1], Songling Huang[1*], *Senior Member, IEEE*, Qing Wang[2], *Senior Member, IEEE*, Shen Wang[1], and Wei Zhao[1]

***Abstract*—The length of the air gap in a negative corona discharge, which affects many corresponding parameters in the discharge process, is of vital importance for the physical investigations. A hydrodynamic drift-diffusion approximation model considering photoionization utilizing finite element method has been used in needle-to-plane air gaps. Trichel pulses, pulse frequency, electron and electric field distribution and surface current density distribution on the anode plate were presented to study the effect of the gap length. An approximate exponential relationship was found to exist between the corona current and the gap length, and also a linear function was found between the pulse frequency and the gap length. The analysis shows that the characteristics of Trichel pulse are strongly dominated by the length of the air gap.**

***Index Terms*—negative corona discharge, exponential fitting, gaps, photoionization.**

## I. Introduction

THE plasma reaction process between the two electrodes with excessive surface curvature difference are more common in the plasma reaction process between the two electrodes with excessive surface curvature difference are more common in the axisymmetric domain and can be self-sustaining in some cases [1]-[6]. Especially for the negative corona discharges, it generates when the inception electric field I achieved in the asymmetric domain like a point-towards-plane electrode configuration and the sharper side performs as the discharge one [7]. In recent years, the study of plasma microscopic physical processes has received more and more attention [8]. In 1985, the periodic current waveform was calculated by Morrow from the simulation for the first time and a simulation model was established by solving a series of coupled equations [9]. Then the model was supplemented in 2000 by Gupta and he found that as the ionization coefficient increases, the rise time of the current pulse decreases gradually [10]. And Sattari used FEM-FCT method to obtain the subsequent pulses by solving the distribution of charged particles [11], [12]. Then continuity equations in the mathematical model were improved and photoionization term was added into the equations, which making the discharge model more accurate than before [13].

The relationship between the long discharge gap and the process of negative corona has been proved to be very close, and considerable work has been done to this issue by many engineers and physicists [14]-[20]. As for the electrode gaps in millimeters, the characteristics of corona electrodes under different discharge gaps was investigated by Iuga using a wire-roll configuration in 2004 and concluded that the corona area under large gaps is much more extensive than small ones [21]. Then in 2008, variations of the voltages and the currents at different gaps were studied by Khaddour. However, further investigations on this phenomenon hadn't been discussed thoroughly [22]. In 2011, Tirumala investigated the positive corona discharges in the sub-millimeter gaps using a wire-plane structure and found that the reduction in the gap length and wire radius will result in an increase of discharge currents [23]. Experimental method was utilized by Ren in 2012 to study positive corona under different gaps and voltages [24]. Then power frequency breakdown voltages of rod-plane gaps were investigated by Qiu in 2015 and he found that the breakdown voltages would increase with the gap length [25]. Overall, relatively little work has been done to analyze the effect of air gap in a negative corona from the aspect of microphysical process, especially for the Trichel pulses.

In previous studies, the effect of the photoionization term was well discussed for negative corona discharges and it led to a conclusion that the photoionization process will weaken the amplitude of the Trichet pulses, and the characteristics of Trichel pulse parameters was also studied [26], [27]. In this paper, an improved simulation model with photoionization term was presented and the fluid dynamics equations coupled with Poisson's equation were calculated to investigate the effect of the gap length in a negative corona discharge in room temperature and standard atmospheric pressure. The relationship between Trichel pulses, pulse frequency, surface current density and electric field was investigated under different gaps.

Correspondence to: Prof. S Huang.
[1]State Key of Power Systems, Department of Electrical Engineering, Tsinghua University, Beijing, 100084, China
[2]Department of Engineering, Durham University, Durham, DH1 3LE, United Kingdom

## II. Model Description

### A. The Governing Equations

The transport process of non-thermal plasmas was calculated by the fluid dynamics equations and Poisson's equation as was done previously, while the source term was corrected by applying photoionization term proved by Tran's experiment [28]. The hydrodynamic drift-diffusion model is shown

$$\frac{\partial c_e}{\partial t} = S_{ph} + c_e\alpha|\boldsymbol{W}_e| - c_e\eta|\boldsymbol{W}_e| - c_e c_p\beta_{ep}, \quad -\nabla\cdot(\boldsymbol{W}_e c_e - D_e\nabla c_e) + S_0 \tag{1}$$

$$\frac{\partial c_p}{\partial t} = S_{ph} + c_e\alpha|\boldsymbol{W}_e| - c_n c_p\beta_{np} - c_e c_p\beta_{ep}, \quad -\nabla\cdot(\boldsymbol{W}_p c_p - D_p\nabla c_p) + S_0 \tag{2}$$

$$\frac{\partial c_n}{\partial t} = |\boldsymbol{W}_e|\eta c_e - c_n c_p\beta_{np} - \nabla\cdot(\boldsymbol{W}_n c_n - D_n\nabla c_n), \tag{3}$$

$$\boldsymbol{E} = -\nabla V, \tag{4}$$

$$-\nabla\cdot(\varepsilon_0\varepsilon_r\nabla V) = -ec_e + ec_p - ec_n, \tag{5}$$

$$I = \left(\frac{\mathrm{d}}{\mathrm{d}t}\int_\Omega \frac{\varepsilon_0\varepsilon_r|\boldsymbol{E}|^2}{2}\mathrm{d}\Omega + \int_\Omega\sum_{e,p,n} ec_i\boldsymbol{W}_i\cdot\boldsymbol{E}\mathrm{d}\Omega\right)\Big/V_a, \tag{6}$$

where the $c_e$, $c_p$ and $c_n$ are the number density of the charged particles, respectively; the ionization $\alpha$, attachment $\eta$, recombination $\beta_{ep}$ and $\beta_{np}$ are the simulation coefficients; the drift velocities are $\boldsymbol{W}_i$; the diffusion coefficients are $D_i$; $S_{ph}$ the production rate of photoelectrons and $S_0$=1.7×10$^9$[1/(s·m$^3$)] the cosmic radiation background ionization; The swarm parameters in Table 1 used in the model were improved by Kang and then proved by Tran and summarized by Georghiou et al [29], [30]; $I$ is the Trichel pulse current and $V_a$ the applied voltage [31]. And $\gamma$=0.004 is utilized in this paper [32].

TABLE 1
VALUE OF THE SWARM PARAMETERS (E IN V CM$^{-1}$)

| Parameters | Value |
|---|---|
| $\alpha$/cm$^{-1}$ | 3500exp (-165000/E) |
| $\eta$/cm$^{-1}$ | 15exp (-25000/E) |
| We/(cm/s) | -6060E$^{0.75}$ |
| Wp/(cm/s) | 2.43E |
| Wn/(cm/s) | -2.70E |
| $\beta$ep/ (cm$^3$/s) | 2x10$^{-7}$ |
| $\beta$pn / (cm$^3$/s) | 2x10$^{-7}$ |
| De/ (cm$^2$/s) | 1800 |
| Dp/ (cm$^2$/s) | 0.11 |
| Dn / (cm$^2$/s) | 0.046 |

The photon generation rate distribution function is shown as the equation [33]-[36].

$$A_j p_{O_2}{}^2 I(\boldsymbol{r}) = \left(\lambda_j p_{O_2}\right)^2 S_{ph}{}^j(\boldsymbol{r}) - \nabla^2 S_{ph}{}^j(\boldsymbol{r}), \tag{7}$$

$A_j$ and $\lambda_j$ are the parameters which fits well in the previous experiment where $j$=1,2,3; and the oxygen's partial pressure $p_{O2}$=150Torr; $I(\mathbf{r})$ the generation rate of photons released in space [36].

### B. Numerical Algorithm

By utilizing COMSOL Multiphysics 5.3a, the fluid equations in this paper were calculated. And the artificial diffusion was utilized to reduce numerical divergence in the model. For the strongly coupled equations, the streamline diffusion method should be used in the whole equation set. It was developed by

Mallet et al and was later lead to GLS applied to the N-S equations [37]-[38]. For control equation of the incompressible flow, the shape function of the pressure should be smaller than the shape function of the velocity. It shows that if the incompressible Navier Stokes equation is stable through streamline diffusion, then it can use equal-order interpolation.

Therefore, streamlined diffusion is essential. As for the diffusion of crosswind type, it will introduce additional diffusion in the sharp boundary layer and shear layer, otherwise it will require a very fine mesh to solve. Crossflow diffusion will make the results easier to obtain. The accuracy of the numerical algorithm has been verified utilizing Morrow&Lowke's and Ducasses et al.'s swarm parameters rather than Kang's swarm parameters in our studies [39]. The conclusion obtained by two simulation methods is that the peak value of the current waveform and the pulse frequency are almost the same.

The initial number density of the electron-positive ion pair has a Gaussian distribution where peak $c_{max}$ of 10$^{16}$m$^{-3}$, width $s_0$ of 25 $\mu$m and $z_0$ is the length of the gap [28].

$$c_{e,p} = c_{max}\times\exp\left[-\frac{r^2}{2s_0^2} - \frac{(z-z_0)^2}{2s_0^2}\right], \tag{8}$$

It was verified that the initial distribution does not affect the discharge process but accelerate the generation of pulses. And the boundary conditions are described in Fig. 1 and Table 2.

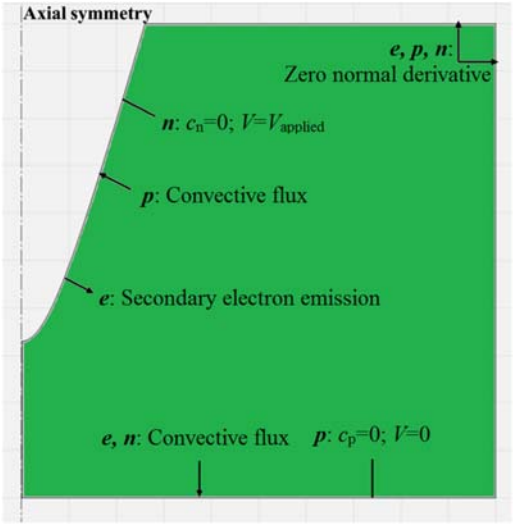


Fig. 1 Boundary conditions of the model

TABLE 2

DESCRIPTION OF THE BOUNDARY CONDITIONS IN THE SIMULATION MODEL ($i$ DENOTES $e$, $p$, $n$, RESPECTIVELY)

| Zero Normal Derivative | Secondary Emission | Zero Normal Derivative |
|---|---|---|
| $\boldsymbol{n}\cdot\left(-D_i\nabla c_i\right)=0$ | $-\boldsymbol{n}\cdot\left(\boldsymbol{W}_e c_e-D_e\nabla c_e\right)=\gamma c_p\left\|\boldsymbol{W}_p\right\|$ | $\boldsymbol{n}\cdot\left(\varepsilon_0\varepsilon_r\boldsymbol{E}\right)=0$ |

## III. RESULTS AND DISCUSSIONS

In this simulation, the applied voltage is -4.7 kV on the needle electrode, and the length of the gap ranges from 2.3 mm to 2.7 mm. The needle tip's radius is fixed into 250 $\mu$m. The gap length of 2.5 mm is chosen as a special case to study the Trichel pulses, electron density distribution and electric field distribution. The Trichel pulse train is shown in Fig. 2(a) and the detail of the third pulse is shown in Fig. 2(b). It is observed from Fig. 2(a) that the first pulse is larger than the following pulses, which can be explained by the fact that there is little negative ion exist before the first pulse. However, the subsequent pulses are produced in similar conditions and show regularity. That is to say, steady Trichel pulses would be built up after an initial ionization avalanche process. Therefore, the third pulse was chosen in Fig. 2(b) to analyze the micro process of the negative corona discharge. Three moments at 10500 ns, 10559 ns and 11000 ns, which can be seen from Fig. 2(b), were selected to study the three phases of electron multiplication, plasma sheath formation and decay process respectively. The distributions of electric field and electron density are shown in Fig. 3(a-c) at different moments while the distribution of the electron density along the symmetry axis is shown in Fig. 3(d).It is observed from Fig. 3(b) that the formation of electrons has reached the critical density and the electric field is strongly distorted by the space charge distribution at 10559 ns. This critical moment (10559 ns while the gap length is 2.5 mm) is relatively important in the process of a negative corona. Therefore, the peak moment of the third Trichel pulse is chosen as the critical moment in Fig. 5-7 under different gap lengths.

It has been proved that the length of the air gap has a significant effect on the discharge process, such as the inception and breakdown voltage. As for the negative corona discharge in this model, the peak of the first pulse and the subsequent pulses under different gaps are shown in Fig. 4, as well as the pulse frequency. It is shown in Fig. 4 that the peak value of the Trichel pulse decrease with the increase of the gap lengths at an applied voltage of -4.7 kV, which fit well with quadratic function. The pulse frequency also decreases with the increase of the gap lengths while approximately proportional to the lengths. The negative corona discharge is a time dependent transient process and the current pulse amplitude is closely related to the electric field, electron density and the drift velocity of the charged particles according to the equation (8). It can be observed from Fig. 3(b) that the peak value of the electron density and the electric field dominates the corona discharge current at the peak moment of 10559 ns, and the electric field distribution is strongly distorted at this moment. As the gap length decreases, the spatial electric field increases (Fig. 6) and the electron impact ionization process will be more intense and the accumulation of p-ions around the cathode enhances the electric field between the plasma sheath and the cathode surface. In addition, the n-ions attached throughout the area will reduce the electric field between the plasma sheath and anode plate. Then the higher number density of the electrons in the ionization region will strengthen the process of ionization. Therefore, the greater the spatial ion flux density, the greater the corona current. The characteristics of the Trichel pulse peak under different gap lengths could also be explained by the surface current density on the anode plate. The surface current density distribution on the plate under different gap lengths is shown in Fig. 5 and it can be observed from the figure that the current density on the plate mainly concentrates in the range from 0 mm to 2 mm in radial direction. And the current density increases with the decrease of the gap length, which leading to the variation of the peak value of the Trichel pulse in Fig. 4. The electric field distribution along the symmetry axis is shown in Fig. 6 and a strongly distorted region could be observed near the cathode. It is interesting to see that the electric field near the anode plate decreases with the increase of the gap length and the electric field starts to rise when getting closer to the anode plate. For a longer gap and lower electric field, the clearance rate of space charge will reduce between the two pulses. That is to say, it will take more time for charged particles to move away from the corona region, and the frequency of the Trichel pulses will decrease as shown in Fig. 4.

The Trichel pulse frequency and the peak value of subsequent pulses are the parameters which should be critically concerned. The subsequent corona current ($I$) can be expressed as (9) and the Trichel pulse frequency can be expressed as (10) in Fig. 7.

$$I=0.87\text{-}0.0078e^{(d-2.3)/0.116}, \tag{9}$$

$$F=759.02\left(2.788-d\right), \tag{10}$$

where $I$ (mA) is the peak value of subsequent pulses; $F$ (kHz) the frequency of the Trichel pulses; $d$ (mm) the length of the air gap.

It is known that the distribution of the electric field (or the cathode's electric potential) is important to the corona current in the discharge process. Therefore, the peak value of Trichel pulses has a strong coupling relationship with the electric field in the ionization region (where ionization dominates attachment). The axial electric field in the hyperboloid-to-plane gap is derived through Eyring's conclusions [40].

$$E\left(0\right)\approx\frac{2V}{\ln\left(4d/r\right)}\frac{1}{r}, \tag{11}$$

Where E(0) is the electric field around the needle tip; $V$ the applied voltage on the needle; $r$ the radius of the needle tip. The equation (11) agrees with the expression given by Loeb *et al* [3]. It can be concluded from the theoretical formula that the electric field $E(0)$ decreases with the increase of the gap length $d$, and there is an exponential relationship between $d$ and $E$. It is shown in (9) that the current peak $I$ decreases with the increase of the gap length $d$. Also, there is an exponential relationship between $d$ and $I$. Therefore, the exponential fitting method is both theoretically and mathematically acceptable.

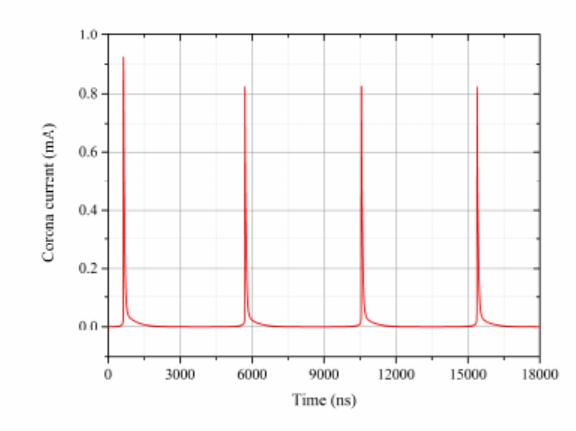


(a) The Trichel pulse train.

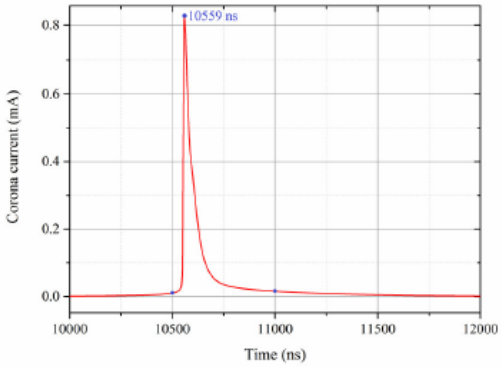


(b) The third Trichel pulse.

Fig. 2. Trichel pulse under applied voltage of -4.7 kv and 2.5mm gap length (a) The Trichel pulse train; (b) The third Trichel pulse.

(b) 10599 ns.

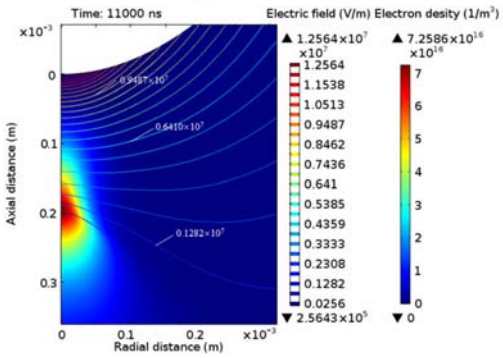


(c) 11000 ns.

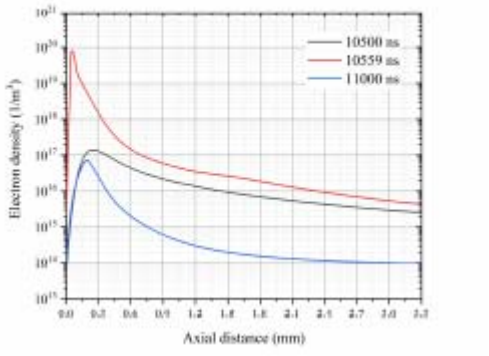


(d)

Fig. 3. Electron density distribution and electric field distribution at three moments: (a) 10500 ns; (b) 10599 ns; (c) 11000 ns; (d) Distribution of the electron density along the symmetry axis.

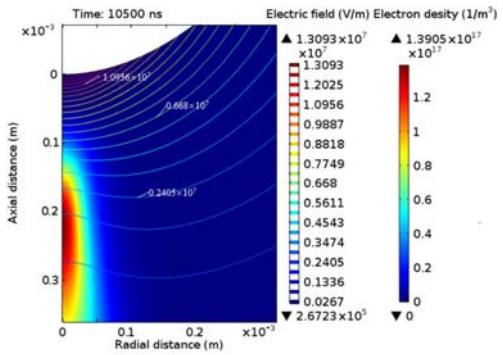


(a) 10500 ns.

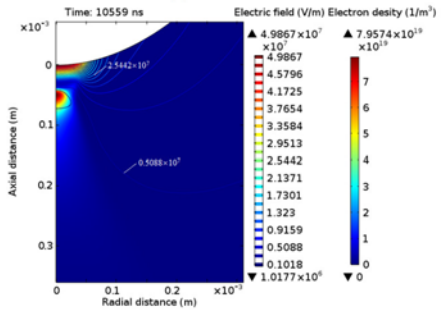


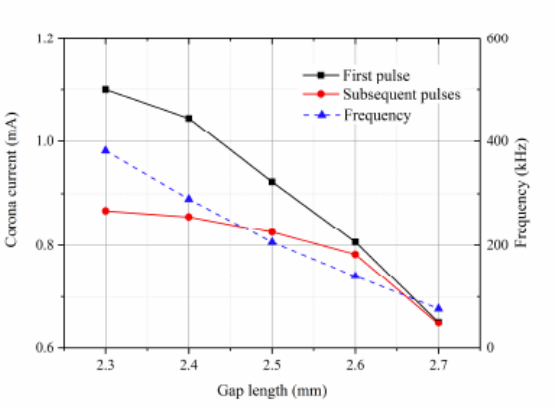


Fig. 4. The peak of the Trichel pulse frequency under different gap lengths.

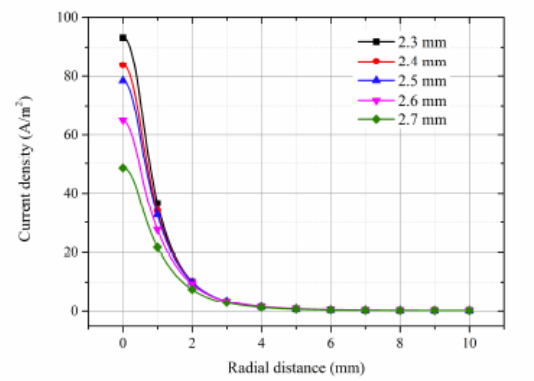


Fig. 5. Surface current density on the anode plate at the critical moment.

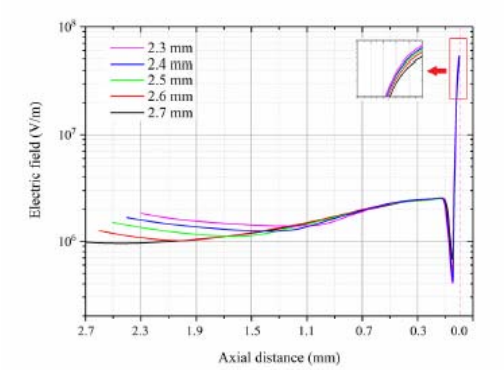


Fig. 6. Electric field distribution along the symmetry axis under different gap lengths at the critical moment (the anode plate is on the left and the cathode is on the right).

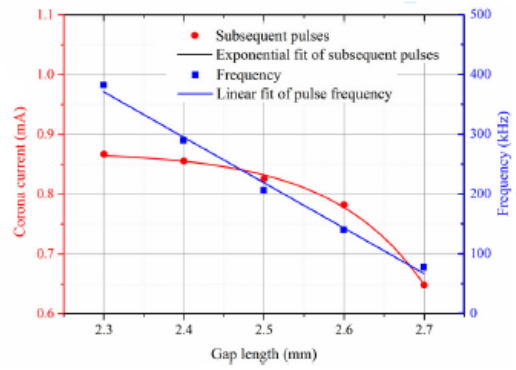


Fig. 7. Fitting curve of subsequent pulses and pulse frequency.

## IV. Conclusion

Negative corona discharge in air under different gap lengths is investigated by 2D axisymmetric finite element model in this paper. Photoionization term is added to the model to improve the accuracy of the calculation. An approximate exponential relationship has been found to exist between the peak of the Trichel pulse and the gap lengths. This phenomenon can be explained by the different distribution of the surface current density on the anode plate under different gap lengths. The variation of the electric field, electron density and positive ion density in strong ionization region and the negative ion density within the whole region also affect the peak of the Trichel pulse at various gaps. And the frequency of the Trichel pulses decreases linearly with the increase of the gap length.

## Acknowledgments

This research was supported by the National Natural Science Foundation of China (NSFC) (No. 51677093) and the National Key Scientific Instrument Development Projects (Grant No. 2013YQ140505).

## References

[1] G. W. Trichel, "The mechanism of the positive point-to-plane corona in air at atmospheric pressure," *Phys. Rev.,* vol. *55*, pp. 382–390, Feb. 1939.

[2]. J. M. Meek, "A theory of spark discharge," *Phys. Rev.,* vol. 57, pp. 733–728, Apr. 1940.

[3]. L. B. Loeb and A. F. Kip, G. G. Hudson, "Pulses in negative point-to-plane corona," *Phys. Rev.,* vol. 60, pp. 714–722, Nov. 1941.

[4]. T. N. Giao and J. B. Jordan, "Modes of corona discharges in air," IEEE Trans. Power App. Syst., vol. PAS-87, pp. 1207–1215, May. 1968.

[5]. W. L. Lama and C. F. Gallo, "Systematic study of the electrical characteristics of the 'Trichel' current pulses from negative needle-to-plane coronas," *J. Appl. Phys.,* vol. 45, pp. 103–113, Jan. 1974.

[6]. R. Morrow and J. J. Lowke, "Streamer propagation in air," *J. Phys. D: Appl. Phys.,* vol. 30, pp. 614–627, May. 1996.

[7]. B. He, T. W. Li, Y. P. Xiu, H. Zhao, Z. R. Peng, and Y. P. Meng, "Study on law of negative corona discharge in microparticle-air two-phase flow media," *AIP. ADV.,* vol. 6, p. 035114, Mar. 2016.

[8]. G. Sansone et al., "Electron localization following attosecond molecular photoionization," *NATURE*, vol. 465, pp. 763–766, Jun. 2010.

[9]. R. Morrow, "Theory of negative corona in oxygen," *Phys. Rev. A,* vol. 32, pp. 1799–1809, Sep. 1985.

[10]. D. K. Gupta, S. Mahajan and P. I. John, "Theory of step on leading edge of negative corona current pulse," *J. Phys. D: Appl. Phys.,* vol. 33, pp. 681–691, Dec. 1999.

[11]. P. Sattari, G. S. P. Castle and K. Adamiak, "Numerical simulation of Trichel pulses in a negative corona discharge in air," *IEEE Trans. Inf. Technol. Biomed.,* vol. 47, pp. 1935–1943, Jul. 2011.

[12]. P. Sattari, G. S. P. Castle and K. Adamiak, "Trichel pulse characteristics—negative corona discharge in air," *J. Phys. D: Appl. Phys.,* vol. 44, p. 155502, Mar. 2011.

[13]. B. X. Lu and H. Y. Sun, "The role of photoionization in negative corona discharge," *AIP. Adv.*, vol. 6, p. 095111, Sep. 2016.

[14]. F. Lv, Y. Ding, D. Fan, Y. Ding, Q. Li, X. Wang, X. Yao, "Characteristics and Altitude Correction of Rod-Rod Long Air Gap Impulse Discharge", *Icheve*. vol. 10, pp. 1109. 2016.

[15]. X. C. Li, H. H. Zhao, P.Y. Jia, W. T. Bao, C. Di, J. Y. Chen, "Characteristics of a large gap uniform discharge excited by DC voltage at atmospheric pressure", *Chin. Phys. B*. vol. 23, pp. 1674. 2014.

[16]. S. Xie, J. Li, T. Luo, Y. Zhang, J. He, C. Wu, Y. Yue, "Formation and Characteristics of Negative Stepped Leaders in 4-10m Long Air Gap Discharges", Iclp. **10**, 1(2016)

[17]. I. Gallimberti, G. Bacchiega, A. Bondiou-Clergerie, P. Lalande, "Fundamental processes in long air gap discharges", *C. R. Physique.* vol. 3, pp. 1335-1359 (2002)

[18]. K. Takaki, H. Akiyama, "Induction of Long Gap Discharge by Water Jet", *IEEE T Plasma Sci*. **36**, 1148-1149. 2008.

[19]. O. Diaza, L. Arevalo, V. Cooray, "Parameter variation in leader channel models used in long air gap discharge simulation.", *Electr Pow Systrem*. vol. 139, pp. 32-36. 2016

[20]. F. F. Wu, R. J. Liao, K. Wang, L. J. Yang, and S. Grzybowski, "Numerical simulation of the characteristics of heavy particles in bar-plate DC positive corona discharge based on a hybrid model," *IEEE Trans. Plasma Sci.,* vol. 42, pp. 868–878, Mar. 2014.

[21]. A. Iuga, A. Samuila, M. Blajan, R. Beleca, R. Morar, L. Dascalescu.

"Characterization of wire corona electrodes at various discharge gaps in electrostatic separation processes", vol. 4, 1969, 2004.
[22]. B. Khaddoura, P. Attena, J.-L. Coulombb, J Electrostat. "Numerical solution of the corona discharge problem based on mesh redefinition and test for a charge injection law", vol. 66, pp. 254-262, 2008.
[23]. R. Tirumala, Y. Li, D.A. Pohlman, D.B. Go, "Corona discharges in sub-millimeter electrode gaps", J Electrostat. vol. 69, pp.36, 2011.
[24]. M. Ren, M. Dong, Z. Ren, H. B. Zhou, A. C. Qiu, "Chaotic Characteristic of Corona Discharge Series in Air Described by a 2D-nonlinear Discrete Dynamic Model", Electrical Review. vol. 88, pp. 11a, 2012.
[25]. Z. B. Qiu, J. G. Ruan, D. C. Huang, Z. H. Pu, "A Prediction Method for Breakdown Voltage of Typical Air Gaps Based on Electric Field Features and Support Vector Machine", *IEEE T Dielect El In*. vol. 22, pp. 4, 2015.
[26]. B. X. Lu, H. Y. Sun, Q. K. Wu, "Characteristics of negative corona discharge in air at various gaps", *IEEE Trans. Plasma Sci.* 45,2191(2017).
[27]. B. X. Lu, H. Y. Sun, Y. Yang and Q. K. Wu, "The role of negative corona in charged particle dynamics," *Simul. Model. Pract. Th.*, vol. 74, pp. 64-79, Feb. 2017.
[28]. T. N. Tran, I. O. Golosnoy, P. L. Lewin, and G. E. Georghiou, "Numerical modelling of negative discharges in air with experimental validation," *J. Phys. D: Appl. Phys.,* vol. 44, p. 015203, Dec. 2010.
[29]. W. S. Kang, J. M. Park, Y. Kim, and S. H. Hong, "Numerical study on influences of barrier arrangements on dielectric barrier discharge characteristics," *IEEE Trans. Plasma Sci.,* vol. 31, pp. 504–510, Aug. 2003.
[30]. G. E. Georghiou, A. P. Papadakis, R. Morrow, and A. C. Metaxas, "Numerical modelling of atmospheric pressure gas discharges leading to plasma production," *J. Phys. D: Appl. Phys.,* vol. 38, pp. R303–R328, Sep. 2005.
[31]. R. Morrow and N. Sato, "The discharge current induced by the motion of charged particles in time-dependent electric fields; Sato's equation extended," *J. Phys. D: Appl. Phys.,* vol. 32, pp. L20–L22, 1992.
[32]. R. Morrow and T. R. Blackburn, "The Role of Photoionization in Streamer Discharge Formation in Voids," *IEEE Trans. Plasma Sci.,* vol. 27, pp. 26–27, Feb. 1999.
[33]. S. Pancheshnyi, M. Nudnova and A. Starikovskii, "Development of a cathode-directed streamer discharge in air at different pressures: Experiment and comparison with direct numerical simulation," *Phys.Rev.,* vol. 71, p. 016407, Jan. 2005.
[34]. W. X. Sima, Q. J. Peng, Q. Yang, T. Yuan, and J. Shi, "Study of the characteristics of a streamer discharge in air based on a plasma chemical model," *IEEE Trans. Dielectr. Electr. Insul.,* vol. 19, pp. 660–670, Apr. 2012.
[35]. A. Bourdon, V. P. Pasko, N. Y. Liu, S. Celestin, P. Segur, and E. Marode, "Efficient models for photoionization produced by non-thermal gas discharges in air based on radiative transfer and the Helmholtz equations," *Plasma. Sources. Sci. T.,* vol. 16, pp. 656–678, Aug. 2007.
[36]. N. Y. Liu and V. P. pasko, "Effects of photoionization on propagation and branching of positive and negative streamers in sprites," *J. Geophys. Res.,* vol. 109, p. A04301, Sep. 2004.
[37]. T. J. R. Hughes and M. Mallet, "A new finite element formulation for computational fluid dynamics: III. The generalized streamline operator for multidimensional advective-diffusive system," *Comp. Meth. Appl.Mech. Engrg.*, vol. 58, pp. 305–328, 1986.
[38]. G. Hauke and T. J. R. Hughes, "A unified approach to compressible and incompressible flows," *Comp. Meth. Appl. Mech. Engrg.*, vol. 113, pp. 389–395, 1994.
[39]. O. Ducasse, L. Papageorghiou, O. Eichwald, N. Spyrou, M. Yousfi, "Critical Analysis on Two-Dimensional Point-to-Plane Streamer Simulations Using the Finite Element and Finite Volume Methods", IEEE Trans. Plasma Sci. vol. 35, pp. 1287(2007)
[40]. Eyring C F, Mackeown S S, Millikan R A. Fields Currents from Points. Phys Rev, vol. 31, pp. 900-909(1928).